Reactivity of Cl Atom with Triple-Bonded Molecules. An Experimental and Theoretical Study with Alcohols

5 AUTHORS, INCLUDING:

Hariprasad Dilip Alwe
University of Mumbai
7 PUBLICATIONS   **11** CITATIONS

SEE PROFILE

Dhanya Suresh
Bhabha Atomic Research Centre
**36** PUBLICATIONS   **232** CITATIONS

SEE PROFILE

Reactivity of Cl Atom with Triple-Bonded Molecules. An Experimental and Theoretical Study with Alcohols

H. D. Alwe, A. Sharma, M. P. Walavalkar, S. Dhanya,* and P. D. Naik

Radiation & Photochemistry Division, Bhabha Atomic Research Centre, Trombay, Mumbai, India 400 085

Ⓢ Supporting Information

ABSTRACT: The reactivities of the Cl atom with triple-bonded molecules were examined by determining the rate coefficients of reactions of four triple-bonded alcohols (TA), namely, 2-propyn-1-ol, 3-butyn-1-ol, 3-butyn-2-ol, and 2-methyl-3-butyn-2-ol, using the relative rate method, at 298 K. The rate coefficients (k) of reaction of the four alcohols with Cl vary in the range $(3.5-4.3) \times 10^{-10}$ cm^3 molecule^{-1} s^{-1}. These values imply significant contribution of the Cl reaction in the tropospheric degradation of TAs in the conditions of the marine boundary layer. A striking difference is observed in the reactivity trend of Cl from that of OH/O$_3$. Although the reactivity of OH/O$_3$ is lower with triple-bonded molecules, as compared to the double-bonded analogues, the reactivity of the Cl atom is similar for both. For a deeper insight, the reactions of Cl and OH with the simplest TA, 2-propyn-1-ol, are investigated theoretically. Conventional transition state theory is applied to compute the values of k, using the calculated energies at QCISD and QCISD(T) levels of theory of the optimized geometries of the reactants, transition states (TS), and the product radicals of all the possible reaction pathways at the MP2/6-311++G(d,p) level. The k values calculated at the QCISD level for Cl and the QCISD(T) level for OH reactions are found to be very close to the experimental values at 298 K. In the case of the Cl reaction, the abstraction of α-H atoms as well as the addition at the terminal and middle carbon atoms have submerged TS and the contribution of the abstraction reaction is found to be significant at room temperature, at all levels of calculations. Addition at the terminal carbon atom is prominent compared to that at the middle carbon. In contrast to the Cl reaction, only addition at the middle carbon is associated with such low lying TS in the case of OH. The individual rate coefficients of addition and abstraction of OH are lower than that of Cl. The negative temperature dependence of the computed rate coefficients in the temperature range 200−400 K shows that the difference in the TS energy of Cl and OH affects the pre-exponential factor more than the activation energy.
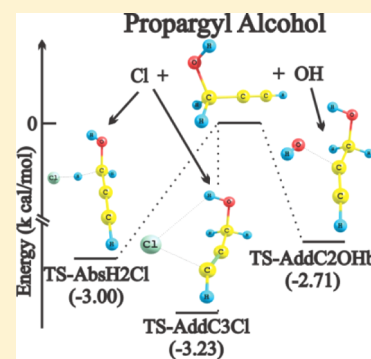
1. INTRODUCTION

A major part of the organic molecules released to the troposphere from anthropogenic and biogenic sources are removed via oxidative degradation reactions, mostly initiated by OH radicals. Reactions of ozone, Cl and NO$_3$ are also important, depending on the chemical nature of the molecule, location, and time. Because the reaction rates with these oxidative species are required for estimating the tropospheric lifetimes, considerable effort has been put in experimentally measuring the rate coefficients of the primary reactions by different methods, theoretically estimating them as well as in developing predictive structure activity relations (SARs). Of these, the most studied reaction is that with OH, for which Atkinson et al.[1,2] have developed a SAR, applicable to most of the classes of organic molecules. The trends in the reactivity of the molecules have been examined in terms of the interacting frontier orbitals, HOMO of the molecule and LUMO of the major tropospheric oxidizing species, namely, OH, NO$_3$, and O$_3$, and SARs have been developed on this basis also.[3,4] Reaction with Cl atoms has been identified as an additional pathway for many organic molecules, in the conditions of marine boundary layer[5] and polluted urban atmosphere, and recently a large atomic chlorine source has also been inferred

from midcontinental reactive nitrogen chemistry.[6] This has led to an increased interest in determining the rate coefficient of the Cl atom with different VOCs. The rate coefficients of the Cl atom with most of the hydrocarbons are larger than that of OH, reaching the diffusion control limits, except in some halogen-substituted molecules.

Recently we have measured the rate coefficients of reactions of Cl atoms with a number of cyclic and linear unsaturated hydrocarbons and both saturated and unsaturated cyclic ethers.[7−11] The attempt to correlate these rate coefficients with the HOMO energy of the reactants showed that unlike the case of reactions of OH, the correlation of the reactivity of the Cl atom is not very good, especially when different functional groups are considered together.[11] This highlights the difference in the primary interactions of OH and Cl, even though the reaction mechanisms of both are known to be similar. The possibility of an addition reaction may make the correlation in unsaturated molecules more complex. Interestingly, among unsaturated molecules, the reactivity of triple-bonded molecules

with electrophiles[12] and with ozone[13] has been noted to be lower than that of the double-bonded molecules, and recently the activation energies of electophilic addition to a triple bond have been shown to be consistently higher than that of the double bond.[14] The experimental studies on the reactivity of triple-bonded molecules with Cl atoms are very limited, and there is no clear understanding of the relative reactivity of the double-bonded and triple-bonded molecules. The reactivity of Cl with ethyne and propyne are less than that of ethene and propene, whereas the reactivity of 1-butyne is more than that of 1-butene.[15] In this perspective, experimental and theoretical investigations on the reactivity of the Cl atom with triple-bonded alcohols (TA) were initiated, to confirm the trend in their reactivity as compared to that for their double-bonded analogues, and also to understand the role of Cl reaction in their tropospheric degradation. The molecules studied are two primary alcohols, namely, 2-propyn-1-ol, also known as propargyl alcohol (PA) and 3-butyn-1-ol (3B1OL), and two secondary alcohols, 3-butyn-2-ol (3B2OL) and 2-methyl-3-butyn-2-ol (2M3B2OL).

Triple-bonded alcohols are widely used in industry as a reactant/chemical intermediate, corrosion inhibitor, solvent stabilizer, soil fumigant, polymer modifier, etc., and they are released to the atmosphere by rapid volatilization from soil and water. A report submitted under the US EPA HPV Challenge Program on the simplest of them, 2-propyn-1-ol, predicts a half-life of 12 h for this molecule in the troposphere, which is based on the rate coefficient of its reaction with OH, estimated using AOPWIN.[16] Although the tropospheric reactions of many double-bonded alcohols of biogenic origin have been studied recently, there is only a single study on the triple-bonded alcohol, where the rate coefficient of the reaction of OH with PA at room temperature has been determined by the LP-LIF method at a pressure of 10−20 Torr.[17] This value is found to be lower than that of allyl alcohol under the same condition. The rate coefficients of the reactions of triple-bonded alcohols with ozone are also not known and an attempt was made to determine the same.

2. EXPERIMENTAL AND COMPUTATIONAL METHODS

2.1. Rate Coefficient Measurements. Rate coefficients at room temperature (298 ± 2 K) were determined using the relative rate method, where the rate of decrease in the concentration of the TAs due to their reactions with the atmospheric oxidant, X, is compared to that of a reference molecule (R), with known rate coefficient.

$$TA + X \rightarrow products \tag{1}$$

$$R + X \rightarrow products \tag{2}$$

Assuming that TA and R react only with the reactant X, the fractional loss of TA and R are related by the standard expression,

$$\ln\left[\frac{[TA]_{t_0}}{[TA]_t}\right] = \left[\frac{k_X^{TA}}{k_X^R}\right] \ln\left[\frac{[R]_{t_0}}{[R]_t}\right] \tag{I}$$

where $[TA]_{t_0}$, $[TA]_t$, $[R]_{t_0}$, and $[R]_t$ are the respective concentrations at time 0 and t, and k_X^{TA} and k_X^R are the rate coefficients for reactions 1 and 2, respectively. Thus, the plots of logarithms of the ratios of fractional changes in the concentrations of both TA and R at various specific times

give straight line with zero intercept and slope of k_X^{TA}/k_X^R. The rate coefficient k_X^{TA} is calculated using the known value of k_X^R.

The details of the experimental setup and procedure for determining the rate coefficient of the reaction of Cl atom, OH and O_3 is described elsewhere.[9−11] The Cl atom and OH radical are generated in situ by photolysis of CCl_3COCl and H_2O_2, respectively, using monochromatic UV lamps from Rayonett at 254 nm. The quantum yield of OH formed by photolysis of H_2O_2 at wavelengths above 230 nm is considered to be 2,[15] and interference of any other fragment such as HO_2, formed by additional dissociation pathways, is negligible in the present experimental conditions. The negligibly small yields of HO_2 (<0.02) and $O(^1D)$ (0.01) observed from the photodissociation of H_2O_2 at 248 nm[18] further confirm this. Although photodissociation of CCl_3COCl is not so well established as that of H_2O_2, it has been used as a source molecule for Cl atom for most of the Cl reactions with unsaturated molecules[19] and the interference from counter-fragments can be considered to be negligible, because experiments with Cl_2, $SOCl_2$, and CCl_3COCl yield the same values of rate coefficients.[20] Ozone, generated as the O_3/O_2 mixture (<2%) using an ozonizer, was injected at intervals and allowed to react with TA and R. The reactions were carried out in quartz reactors of volume of about 3 L, maintaining a total pressure of 800 ± 3 Torr. The depletion of TA and R was followed, after photolyzing for a fixed time or after addition of ozone, using a gas chromatograph (Shimadzu GC-2014) with a flame ionization detector. The reaction mixture was allowed to reach equilibrium before and after each photolysis, which was confirmed by the reproducibility of the concentration measured during consecutive sampling. The reference molecule R was selected on the basis of the similarity of the rate coefficients (the ratio of the rate coefficients not exceeding 2.5) and the least interference during the gas chromatography analysis, either from the molecule or from the products of their reactions with the oxidants.

Nitrogen gas of purity >99.9% (INOX Air Products Ltd., Mumbai, India) and ultrapure air (Zero grade; Chemtron Science Laboratories, Mumbai, India) were used as buffer gases. High purity oxygen (>99.9% from Alchemie Gases & Chemicals Pvt. Ltd., Mumbai, India) is used to generate ozone/oxygen mixture. PA from Merck (>99%), 3B1OL and 3B2OL from Aldrich (97%), and 2M3B2OL from Fluka (98%) were used for the experiments. Among the reference molecules, *cis*- and *trans*-butenes, 1-butene, *n*-butane, and propane were from Matheson, and all the other reference molecules, as well as tetrahydropyran and tetrahydrofuran, used as OH scavengers, were from Sigma-Aldrich with a purity ≥97%. Samples of the compounds were stored in evacuated glass vessels and subjected to freeze−pump−thaw cycles prior to use.

2.2. Computational Methods. Ab initio theoretical studies were carried out, to calculate the rate coefficients of the reactions of Cl and OH with the simplest triple-bonded alcohol, 2-propyn-1-ol (PA). The geometries of the reactant, transition states (TS) and products of abstraction and addition channels were optimized at the second order Møller−Plesset (MP2) level of theory, with the 6-311++G** basis set. The restricted-open wave function (ROMP2) was applied in all geometry optimizations of radicals to avoid spin contamination (value of $\langle s^2 \rangle$ is very near to 0.75 for all the TS as well as product radicals), and restricted wave function was used for all others. Optimization of the geometry of certain TS and radicals by density functional methods was found to be difficult. ROHF
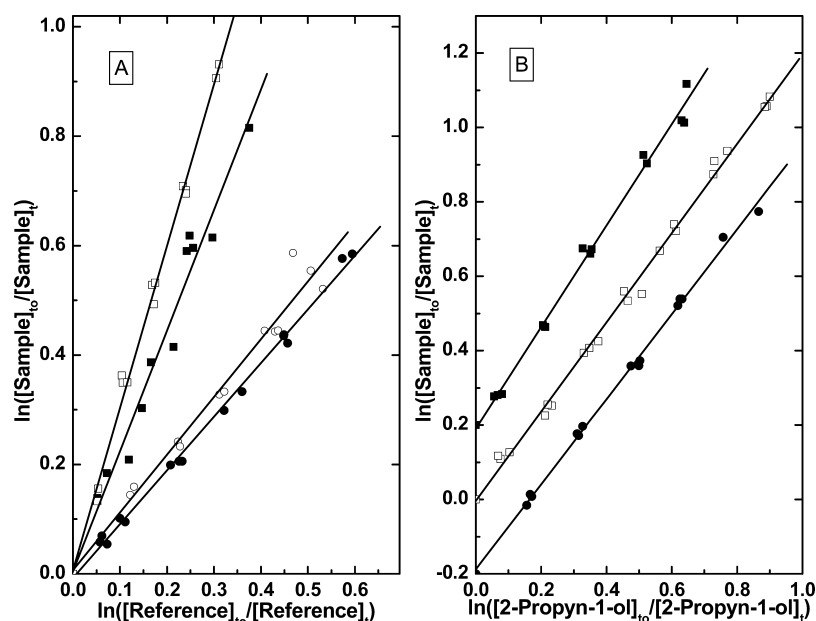
Figure 1. Typical plots of the fractional decrease in the concentration of TAs due to reaction with Cl atom. (A) Relative to different reference molecules: (○) PA with 1-butene, (■) 3B1OL with butane, (□) 3B2OL with propane, and (●) 2M3B2OL with *n*-hexane. (B) Relative to PA: (■) 3B1OL, shifted on the *Y*-axis by 0.2, (●) 3B2OL, shifted on the *Y*-axis by −0.2, and (□) 2M3B2OL.

and ROMP2 methods are reported to give the correct geometry of alkynyl radicals, with the calculated bond energies based on these geometries being comparable to that calculated by M06 method.[21] The harmonic vibrational frequencies were calculated for each structure to verify the nature of the stationary point. The TS was identified by confirming the presence of only one imaginary frequency and all other stationary points were with real frequencies. The addition and abstraction TSs were also confirmed by the normal mode of analysis, that the imaginary frequencies in TS correspond to the stretching modes of the C=C, along with forming O—C/Cl—C bonds (in addition reactions) and the stretching modes of the breaking C—H with forming O—H/Cl—H bonds (in abstraction). All the structures and normal modes of vibrations were viewed in MacMolPlt.[22] The existence of TS on the potential energy surface is further ascertained by intrinsic reaction coordinate (IRC) calculations.

Single point energies of reactants, TS, and products have been computed at quadratic configuration interaction, with single, double, and triple excitations (QCISD(T)) level on geometries optimized at MP2 level with the 6-311++G** basis set. Relevant zero-point energies at the MP2 level have been considered while calculating the final values of QCISD energies. This dual level procedure is known to produce reliable kinetic results while studying similar reactions.[23,24] All MP2 optimizations and IRC calculations were conducted using the GAMESS[25] program package and single-point calculations were carried out using the Gaussian[26] program. Interconversion of chemical structures between these two formats was done by using Open Babel[27] program.

The rate coefficients for reactions were calculated by using conventional transition state theory (TST),[28] given by the following expression:

$$k(T) = \sigma_r \Gamma(T) \frac{k_B T}{h} \left(\frac{Q_{\ddagger}}{Q_R} \right) \exp\left(\frac{-\Delta E^{\ddagger}_0}{RT} \right)$$

(II)

where σ_r is the reaction path degeneracy, $\Gamma(T)$ is the tunneling correction factor, ‡ represents the transition state, k_B is the Boltzmann constant, and h is Planck's constant. T is the temperature in Kelvin, $Q_{\ddagger}$ and Q_R are the partition functions for the TS and the reactants. $\Delta E^{\ddagger}_0$ is the molar zero-point energy inclusive of the barrier height, and R is the universal gas constant. The tunneling corrections were calculated by using Wigner's method[29] and Eckart's symmetrical and unsymmetrical methods.[30,31] Partition functions were computed under harmonic oscillator (HO) approximations. The total partition function was calculated as a product of the individual partition functions and the translational, rotational, vibrational, and electronic partition functions. The electronic partition function of the OH radical and Cl atom were evaluated by taking the splitting of 139.7 cm⁻¹ in the ²Π ground state of OH[32] and splitting of 881 cm⁻¹ between the ground ²P$_{3/2}$ and excited ²P$_{1/2}$ electronic states of Cl atom[33] into account.

3. RESULTS AND DISCUSSION

3.1. Relative Rate Measurements. The stability of the reaction mixtures with respect to wall losses and dark reactions was examined and found to be satisfactory for about 7−8 h, which is more than the total duration of the experiment. The absorption spectrum of 2-propyn-1-ol does not show any significant absorption at 250 nm,[34] and hence direct photolysis of this molecule is not expected. Although the absorption spectra of 3B1OL, 3B2OL, and 2M3B2OL are not reported, addition of more alkyl groups is not expected to affect the absorption characteristics in the wavelength region above 200 nm. The absence of direct photolysis was confirmed experimentally in all cases. The reactions with each triple-bonded alcohol, as well as the reference molecules were carried out independently, to ensure that the products of the reactions do not interfere with the GC measurement of the concentration of the TAs and the reference molecules. The typical logarithmic plots of the relative decrease in the concentration of PA, 3B1OL, 3B2OL, and 2M3B2OL, against the decrease in the

reference molecules, due to their reactions with Cl atoms, are shown in Figure 1A. The slopes obtained with different reference molecules and the calculated rate coefficients are given in Table 1. Because the values obtained using different

Table 1. Relative Ratios and Rate Coefficients of Reactions of Cl with TAs with Different Reference Molecules, [TA] = 100−200 ppm, [R] = 50−100 ppm, [CCl₃COCl] = 350−650 ppm (Buffer gas, N₂; Total Pressure 800 Torr)[a]

sample	reference molecule	average slope	rate coefficient $k_{298} \times 10^{10}$ (cm^3 $molecule^{-1}$ s^{-1})
propargyl alcohol	1-butene(5)	1.02 ± 0.16	3.27 ± 0.66
	butane(4)	1.81 ± 0.08	3.71 ± 0.48
			3.49 ± 0.66[b]
3-butyn-1-ol	*cis*-butene (5)	1.43 ± 0.16	4.48 ± 0.66
	1-butene (4)	1.02 ± 0.10	3.27 ± 0.53
	butane (3)	2.24 ± 0.14	4.59 ± 0.63
	propargyl alcohol(3)	1.34 ± 0.10	4.68 ± 0.95
			4.3 ± 1.3[b]
3-butyn-2-ol	1-butene(4)	0.97 ± 0.04	3.11 ± 0.40
	propane(3)	2.92 ± 0.08	4.09 ± 0.60
	propargyl alcohol(5)	1.20 ± 0.14	4.19 ± 0.93
			3.8 ± 1.2[b]
2-methyl-3-butyn-2ol	1-butene(7)	0.94 ± 0.12	3.02 ± 0.55
	hexane(3)	0.97 ± 0.08	3.06 ± 0.46
	propargyl alcohol(5)	1.24 ± 0.14	4.33 ± 0.95
			3.5 ± 1.4[b]

[a]k(Cl + n-butane)[15] − (2.05 ± 0.25) × 10⁻¹⁰ cm^3 $molecule^{-1}$ s^{-1}; k(Cl + 1-butene) − (3.2 ± 0.4) × 10⁻¹⁰ cm^3 $molecule^{-1}$ s^{-1} (k determined by Orlando et al.[35] was updated with the above value for n-butane) and k(Cl + n-hexane)[19] − (3.15 ± 0.40) × 10⁻¹⁰ cm^3 $molecule^{-1}$ s^{-1}. [b]Average values in bold type.

reference molecules are found to be varying, the rate coefficients of the three butynols were further confirmed against a common reference, PA (Figure 1B). The average rate coefficients of the four alcohols are found to be similar, in the range (3.5−4.3) × 10⁻¹⁰ cm^3 $molecule^{-1}$ s^{-1}, with 3B1OL having marginally higher value.

Attempts to determine the rate coefficients of these molecules with OH, by similar methods, were not successful, due to negligibly small depletion in these alcohols with respect to the reference molecules that could be tried. The low sensitivity for detection of these alcohols makes higher concentration necessary and the small rate coefficients of these molecules with OH make the reaction of OH with H_2O_2 competitive. This could lead to a small percentage of depletion in the alcohol, which probably is experimentally difficult to observe.

The reaction of PA with ozone was also investigated, with ethylene as the reference molecule, which has a rate coefficient of 1.6×10^{-18} cm^3 $molecule^{-1}$ s^{-1}.[15] The depletion in the TAs was very low, with relative ratios of depletion of TAs less than 0.1. This implies that the rate coefficients for the reaction of O_3 with TAs are less than 1×10^{-19} cm^3 $molecule^{-1}$ s^{-1}, the expected range being 1×10^{-20} cm^3 $molecule^{-1}$ s^{-1}, as observed in the case of ethyne and propyne. The rate coefficients of reactions of ozone are known to be dependent on the number

of substituents, position of unsaturation, etc. and may vary significantly for the four TAs considered here. To obtain details regarding this, the relative ratios with respect to PA were measured, as shown in Figure 2. The relative ratios are 1.1 ± 0.08, 0.86 ± 0.02, and 0.79 ± 0.04 for 3B1OL, 3B2OL, and 2M3B2OL respectively.
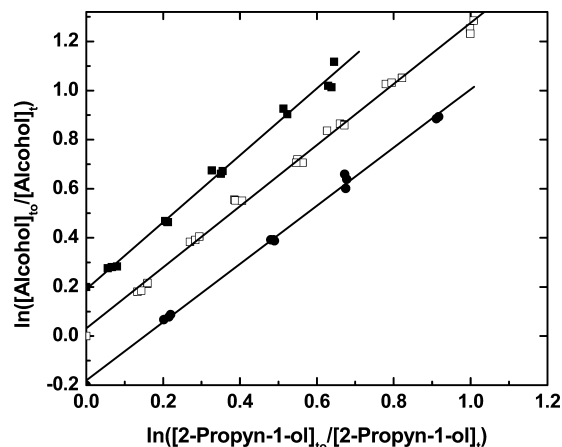
Figure 2. Typical plot of the fractional decrease in the concentration of TAs with that of PA, due to the reaction with O_3 at 298 ± 2 K in air, (■) 3B1OL, shifted on the Y-axis by 0.2, (●) 3B2OL, shifted on the Y-axis by −0.2, and (□) 2M3B2OL.

The rate coefficients of reaction of the triple-bonded and their analogous double-bonded alcohols with Cl and OH are listed in Table 2, along with some additional molecules. Rate coefficients of reactions of ozone are also listed for a comparison of the trends in reactivity. There is only a single report on the rate coefficient of OH with PA,[17] carried out at a pressure range of 10−20 Torr, whereas there are many reports on allyl alcohol, ranging from 3.7×10^{-11} to 6.7×10^{-11} cm^3 $molecule^{-1}$ s^{-1}, the average being 5×10^{-11} cm^3 $molecule^{-1}$ s^{-1}. However, for a comparison with the rate coefficient of PA, the value measured using the same method and conditions[17] is given in the table. Considering the reported value of k_{OH} of PA as a typical value for the triple-bonded alcohols, the values of k_{Cl} are invariably higher than those of k_{OH}, more than 1 order of magnitude higher in triple-bonded molecules, and 5−10 times higher in double-bonded molecules. The reactivity of the triple-bonded molecules with OH is found to be much lower than that of their double-bonded analogues, whereas reactivity of the Cl atom is higher with triple-bonded molecules, except in very small molecules like ethyne and propyne. In the case of reactions of ozone with these TAs, absolute rate coefficients are not known, but their relative ratios with respect to PA are given for comparison. The large variation in the reported rate coefficients of ozone reaction with allyl alcohol, compiled in the table, does not allow a similar comparison of the trend in the double-bonded molecules, to see the substituent effects. However, it is clear that k_{O_3} values of the triple-bonded molecules studied here are at least 2 orders of magnitude lower than their double-bonded analogues. Also, the distribution of k_{O_3} of these TAs is much narrower compared to the variation in the analogous double-bonded molecules. The values of k_{OH}, k_{O_3}, and k_{Cl} listed here imply a higher contribution of Cl atom reaction in the tropospheric degradation of TAs, as compared to the cases of their double-bonded analogues.

Table 2. Rate Coefficients (cm^3 $molecule^{-1}$ s^{-1}) of Reactions of Cl and OH with Some Triple-Bonded Molecules and Analogous Double-bonded Molecules

molecule	$k_{OH} \times 10^{12}$	$k_{Cl} \times 10^{10}$	$k_{O_3} \times 10^{20}$	molecule	$k_{OH} \times 10^{12}$	$k_{Cl} \times 10^{10}$	$k_{O_3} \times 10^{20}$
acetylene	0.75[15]	0.52[15]	1.0[15]	ethylene	7.8[15]	1.0[15]	160[15]
propyne	3.1[15]	2.2[19]	1.43[19]	propene	29[15]	2.7[15]	1000[15]
1-butyne	8.3[19]	3.9[19]	1.97[19]	1-butene	31[15]	3.2[a]	960[15]
2-propyn-1-ol	9.2[17]	**3.5**	< 10	allyl alcohol[b]	37[17]	2.9[19,36]	1100−1800[19]
			1.0[c]		50[19]		
3-butyn-1-ol		**4.3**	<10	3-buten-1-ol	55−59[19]	2.63[37]	620[38]
			1.1 ± 0.08[c]			3.63[38]	
3-butyn-2-ol		**3.8**	<10	3-buten-2-ol	59[39]	3.0[36]	1630[19]
			0.86 ± 0.02[c]			1.44[40]	
2-Me-3-butyn-2-ol		**3.5**	<10	2-Me-3-buten-2-ol	39−6.6[19]	2.13[19,36,40]	863[19]
			0.79 ± 0.04[c]			−4.72	

[a]See footnote in Table 1. [b]The average rate coefficient for the reaction of OH with allyl alcohol is 5×10^{-11} cm^3 $molecule^{-1}$ s^{-1}.[19] However, the value from ref 17 is shown separately to compare with the only reported rate coefficient of PA, under the same condition. [c]Relative ratio of k_{Cl} of the molecule to k_{Cl} of PA, obtained experimentally.

3.2. Theoretical Calculations. To understand the apparent difference in the reactivity trend of triple-bonded alcohols with OH and Cl, a theoretical study was carried out so that the major reaction pathways in both cases can be identified and compared. With the advances in computational chemistry, theoretical *ab initio* calculations are capable of estimating the kinetic parameters of many reactions, very close to the experimental values and this can provide parameters of individual channels, useful for comparing the reactivity trends. Moreover, in addition to Arrhenius parameters, the nature of the transition states involved in the reactions of OH and Cl reactions also may lead to a better understanding of the similarities and difference of the two reactions. The results of the computational study of the different transition states involved in the abstraction of each H atom and addition to both the triple-bonded carbon atoms are discussed below.

3.2.1. Optimisation of Geometry of Reactants and Transition States. PA can exist in either gauche or trans form, depending on the orientation of the OH group with respect to the C−C−C chain. Experimental studies on rotational spectrum[41] as well as theoretical calculations[42,43] confirm that only gauche form is present at room temperature. Our present calculations also show that the gauche form, where the H atom of OH is toward the C−C−C chain, as shown in Figure 3a, is the structure with lowest energy, which is very similar to that reported earlier at MP2/6-31++G** level.[42] This structure, with 4 H atoms, marked as H1, H2, H3, and H4, as shown in Table 3, was considered in further calculations. The structures of the important transition states, listed in Table 3, along with the products of abstraction and addition channels of the reaction of Cl with PA, are shown in Figure 3 as TS and P. Similar structures for reaction of OH are shown in Figure 4.

Among the four H atoms, only abstraction of H2 and H3 were significant, for both Cl and OH reactions. Although H2 and H3 are oriented differently with respect to the C−O−H group, abstraction of both resulted in similar structures of TS for Cl as well as OH reactions. The two TS in the case of Cl atom reaction, AbsH2Cl and AbsH3Cl, are shown in Figure 3, and the energies are listed in Table 3. It can be seen that both are mirror images, with same energy. Hence, only one TS structure, AbsHOH, is shown in the case of OH.

Addition is possible at C2 and C3 positions. Because the orientation of alcoholic O−H makes the molecule unsymmetric, the possibility of approach of Cl atom/OH from

different directions were considered, which resulted in more than one type of TS in some reactions. Thus, two different TS were optimized for addition of Cl and OH at C2, approaching from either the direction of alcoholic OH or from the opposite side. Most of the other directions of approach optimized to either the same or very similar structures with higher energy as those shown in Figure 3 and 4, or did not give any optimized TS. The TSs, where the approaching OH/Cl is opposite to the alcoholic OH group are designated with suffix a and those approaching from the same direction as the alcoholic OH group are designated with suffix b. The imaginary frequencies associated with the TS are listed in Table 3, which were confirmed to be associated with the breaking and forming of bonds in the TS. The IRC calculations also confirm that the optimized TSs connect the reactants and the products.

The bond lengths and interatomic distances are also marked in Figures 3 and 4. It can be seen that the bond length of C≡C is not affected much, but the adjacent C—C bond length changes to 1.43 Å from 1.47 Å in AbsH2Cl and AbsH3Cl (Figure 3). The C—H bond length is changed to 1.34 Å (Figure 3), indicating 23% elongation compared to the original C—H bond. Compared to this, the length of the forming Cl—H bond is only 17.8% more than that in the product H—Cl (1.5 Å compared to 1.27 Å), indicating the TS structure to be more toward the product. These characteristics are very different from the TS for abstraction of H atom, optimized in the case of reaction of Cl atom with double-bonded alcohols (1-pentenol), which is reactant-like with an imaginary frequency of 110i.[23] A similar structure could be optimized in the present case also, with a TS energy of 3.26 kcal/mol at the MP2 level of calculation, which is higher than that of AbsH2Cl, shown as AbsH2Cla in Table 3 and Figure 3. However, the vibration corresponding to the imaginary frequency (670.4 cm^{-1}) in AbsH2Cla is not the simple C—H and H—Cl stretch, as in the case of AbsH2Cl but involves other carbon atoms also. Hence, only AbsH2Cl/AbsH3Cl are considered as the TS for abstraction channel, not AbsH2Cla and AbsH3Cla. The elongation of alcoholic O—H bond observed in AbsH2Cl/AbsH3Cl appears to be due to the change in the C—O bond, following the partial sp^2 nature of the carbon atom, and not due to hydrogen bonding, because the Cl atom is far from the H atom of the hydroxyl group.

In all the addition TSs the length of C≡C bond varies from 1.230 to 1.233 Å, with negligibly small elongation of 1.3% with
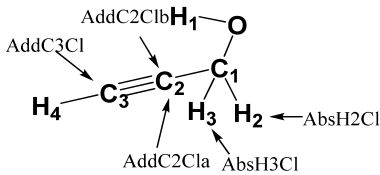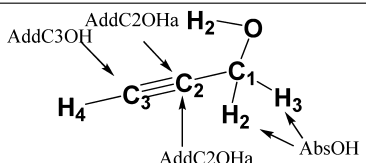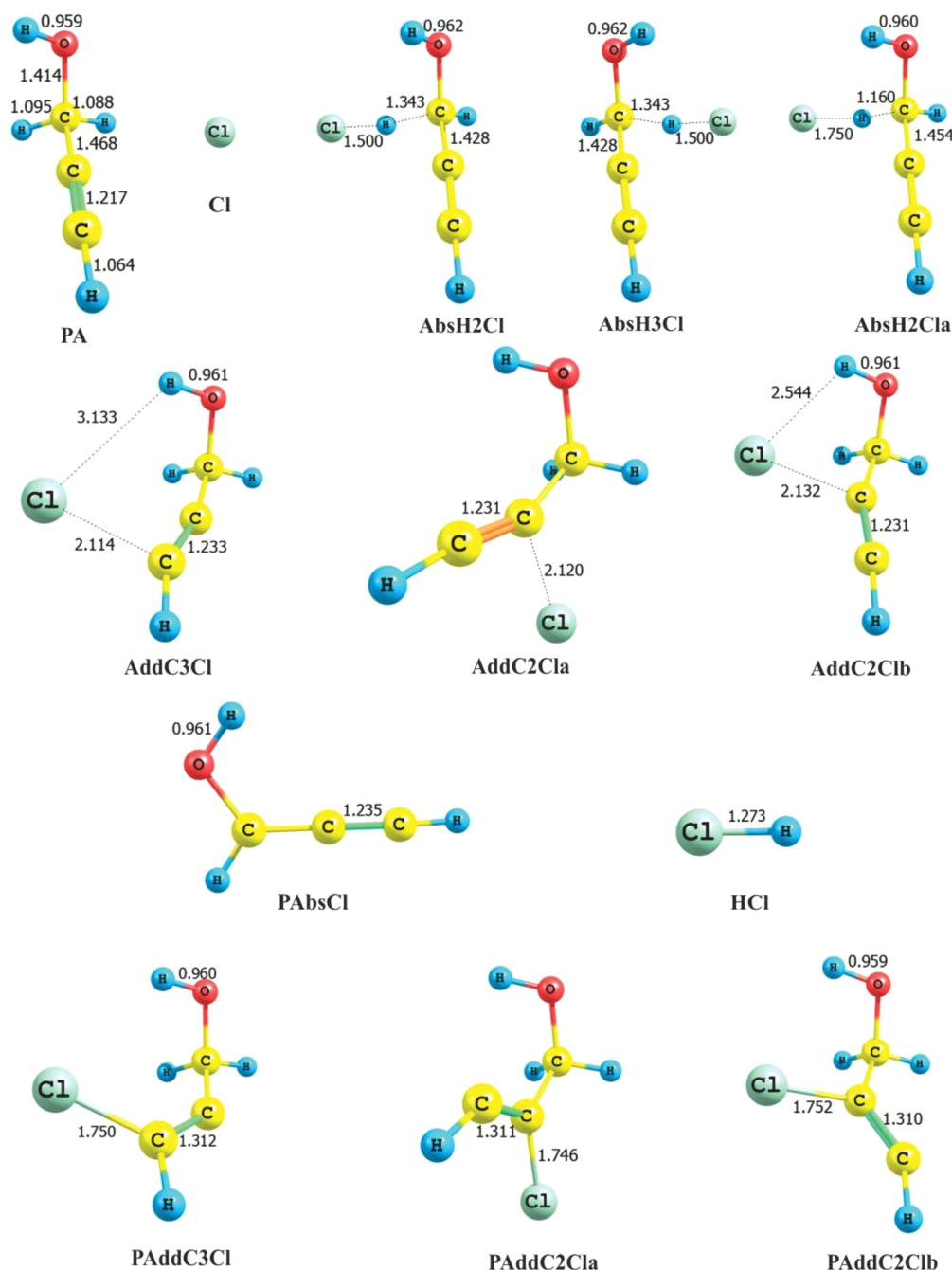
Figure 3. Optimized geometries of the reactants, transition states, and products during the reaction of PA with Cl atom.

respect to the parent molecule (1.217 Å) and the C—Cl distances are near 2.12 Å, which is about 20% longer than the C—Cl distance in the product. This indicates the TS to be very similar to the reactant. No significant change is observed in the alcoholic O—H bond in the addition TSs, implying not much influence of hydrogen bonding with Cl atom.

With respect to the abstraction channel of OH reaction, it can be seen in Figure 4 that the partially broken C—H bond distance in the TS, AbsHOH, is 1.178 Å, very close to that in the reactant molecule (percentage elongation is 8.1%), whereas the length of the H—O bond to be formed is large, 1.353 Å, with a percentage difference of 41.7%. This indicates a reactant like TS, contradicting with the situation in H abstraction by Cl atom. Addition of OH is possible on the middle carbon (C2) as well as the terminal carbon (C3). Although two TS geometries

were optimized with OH approaching from the same side as alcoholic OH at C3, they were very similar, with a marginal difference in the orientation of the H of approaching OH toward the C≡C bond. Of the two, the one with lower energy is considered here. The bond length of C≡C is not affected in the abstraction TS but marginally increases to above 1.23 Å in all the addition TS except in AddC2OHb, where the bond length is only 1.225 Å. The distance of the approaching O atom from the C atom, where addition takes place, is also found to be the lowest in AddC2OHb, only 1.81 Å, whereas in all others it is above 1.98 Å. From Table 4, it can be seen that this TS is of the lowest energy, although the bond lengths shown in Figure 4 show this TS to have a weaker hydrogen bond between the approaching O atom and H of the alcoholic group than that in

Table 3. Details of the Transition States Optimized for Individual Reaction Channels

Structures	TS names	Imaginary frequency (cm^{-1})
	AbsH2Cl	985.41
	AbsH3Cl	986.39
	AbsH2Cla	670.4
	AddC2Cla	1078.29
	AddC2Clb	970.83
	AddC3Cl	1024.83
	AbsOH	2345.48
	AddC2OHa	622.21
	AddC2OHb	2154.19
	AddC3OH	705.61

AddC3OHb, indicated by the elongation of the alcoholic O—H group.

3.2.2. Energy of the Transition States. The energies of TS and products of all the relevant abstraction and addition channels, with respect to the reactants, are calculated at MP2, QCISD and QCISD(T) levels. These energies, including zero point corrections, are shown in Tables 4 and 5 for reactions of Cl and OH, respectively. The relative energies for each TS vary at different levels of theory. For both OH and Cl, the TS for the addition reaction have the lowest energy at all levels, before zero point correction (Table 4). But, for Cl reactions, the TS energy of abstraction becomes equal to or less than that of addition after zero point correction, whereas the addition reaction remains the lowest energy channel of OH reactions, at all levels of calculation. Among the TS optimized for different addition channels of OH reaction, the TS for addition at the middle carbon has the lowest energy, which is also the only TS with energy, lower than that of the reactants. But in the case of Cl, additions at middle and terminal carbon atoms are comparable at QCISD(T) levels of calculations. The heat of the reaction (ΔH) is more negative for OH reactions. Although the exothermicities of Cl addition at middle and terminal carbon atoms are similar, the exothermicity of OH addition at the middle carbon is found to be more than that at the terminal position.

The energies of TS calculated at all levels are very small or lower than that of the reactants, especially in the case of Cl reactions, indicating formation of prereactive complexes as in the case of reaction of OH with allyl alcohol.[44] However, such a prereactive complex, which bifurcates to addition and abstraction channels, could not be optimized in the present study for both Cl and OH. Attempts to optimize such complexes using the terminating geometry of IRC calculations were made from all the important TS mentioned above. In the case of the Cl reaction, a prereactive complex could be optimized only from TSAddC2, which is shown in Figure 5A. Although the energy of this complex is lower than the energy of the TS for abstraction and addition at the MP2 level of calculation by 6.5 and 3.8 kcal mol^{-1}, the energies calculated at QCISD and QCISD(T) levels of calculation are +1.2 and −0.7 kcal mol^{-1}, respectively, both higher than the TS energies for any of the channels, given in Table 4. Moreover, the energy at QCISD level is higher than that of the reactants. Thus, it is

clear that the located complex is not the correct prereactive complex for Cl reaction. In the case of reaction of OH, a prereactive complex as shown in Figure 5 could be optimized from TSAddOHC2. The calculated energies are −3.2 and −5.1 kcal mol^{-1}, at QCISD and QCISD(T) levels, respectively. Unlike the Cl reaction, the same structure was obtained for the abstraction reaction also, but no complex could be obtained for addition at the terminal carbon atom. In many unsaturated molecules such as allyl alcohol, a single prereactive complex is identified for addition, with the OH group at the center of the double bond, which gives two TS corresponding to addition at the two carbons. Thus, the prereactive complexes located for OH reactions also appear to be ambiguous.

3.2.3. Calculation of Rate Coefficients. The rate coefficients for all the channels of reactions of Cl with PA at 298 K, calculated using the TS energies at QCISD and QCISD(T) levels are summarized in Table 6. Because a correct prereactive complex could not be located, and the barrier height is not known, tunneling corrections using Eckart's symmetrical and unsymmetrical potentials could not be applied. Wigner's tunneling correction, which considers only the value of imaginary frequency, is attempted for comparison, as given in Table 6. However, these values are not considered for any further discussion.

The calculated total rate coefficients with QCISD energies without any tunneling corrections, 6.53×10^{-10} cm^3 molecule^{-1} s^{-1}, is found to be close to the experimental value of 3.5×10^{-10} cm^3 molecule^{-1} s^{-1}. This has contribution from addition of Cl at the terminal carbon atom, abstraction of H atoms, as well as a small contribution from addition at the middle carbon atom, almost 10 times less than that at the terminal carbon atom. Considering the possibility of abstraction of two hydrogen atoms, the rates of addition and abstraction are almost similar at room temperature. The calculation with QCISD(T) energies overestimates the value of k_{Cl} by 2 orders of magnitude and H abstraction reaction becomes more dominant than addition. In any case, abstraction is not negligible in the Cl reaction and k for addition at the terminal carbon is more than that at the middle carbon. The presence of 2-propynal as a product (discussed later) also supports the occurrence of an abstraction reaction.

The rate coefficients of the reactions of OH with PA, calculated in a manner similar to that above, using energies at
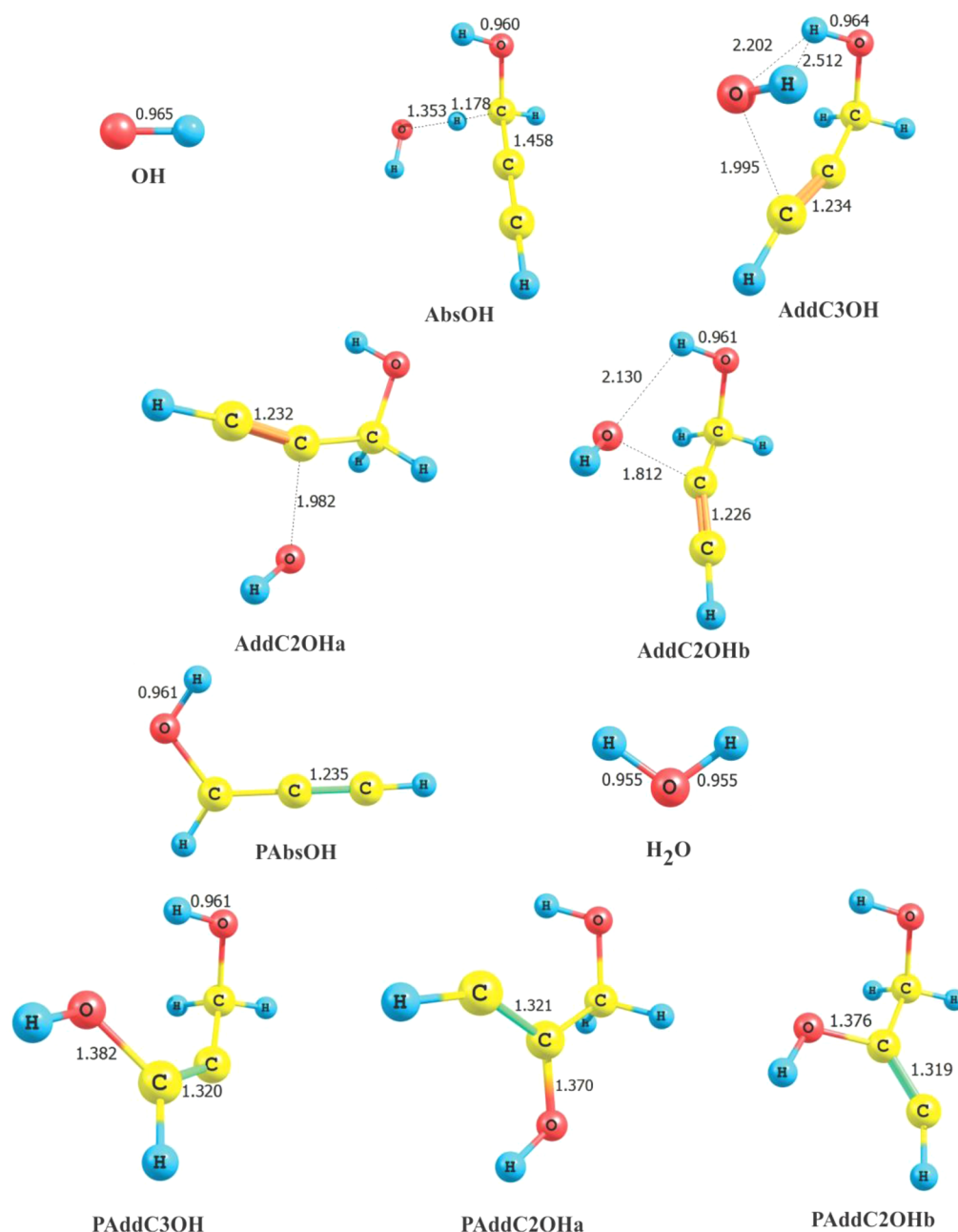
Figure 4. Optimized geometries of the reactants, transition states, and products during the reaction of PA with OH.

the QCISD and QCISD(T) level, without any correction (OH) and with Wigner tunneling correction (WTC) are shown in Table 7. Unlike the Cl reaction, the values show the reaction to be dominated by addition at the middle carbon, which has the lowest TS energy and highest exothermicity among the different addition possibilities. Although the exothermicity of abstraction reaction is close to that of addition, the contribution of abstraction to the overall rate constant is negligibly small. The calculations using QCISD energies are found to underestimate the rate coefficient values and that calculated at the QCISD(T) level, with Wigner tunneling correction (WTC), is found to be the closest to the experimental value of 9.2×10^{-12} cm^3 molecule^{-1} s^{-1}.

Although the nature of the prereactive complex is not confirmed, Eckart's symmetrical and unsymmetrical corrections were carried out, considering the complex shown in Figure 5B

to be the prereactive complex for all the channels. The calculated values, with QCISD and QCISD(T) energies are also included in Table 7. The values of k_{OH}, calculated with QCISD energies are lower by an order of magnitude, but that at the QCISD(T) level is of the same order as the experimental value. Addition at C3 is found to be negligible in all cases. However, with corrections using the Eckart unsymmetrical potential, the contribution of abstraction becomes higher, almost the same as that of addition at the second carbon atom. The calculated k_{OH} at the QCISD(T) level with Eckart's unsymmetrical correction is very close to the experimental value. However, considering the uncertainty in the nature of the prereactive complex, the rate coefficient calculated on the basis of QCISD(T) energy with Wigner's tunnelling correction is considered in further discussion.

Table 4. Relative Energies of Different Transition States (TS) and the Corresponding Products, Calculated for the Cl + PA Reaction[a]

TS	TS energies (kcal mol⁻¹)			product energies (kcal mol⁻¹)		
	MP2	QCISD	QCISD(T)	MP2	QCISD	QCISD(T)
AbsH2Cl	−0.63	0.65	−1.83	−6.84	−10.20	−10.73
	−4.27	−3.00	−5.45	−11.34	−14.70	−15.24
AbsH3Cl	−0.63	0.65	−1.83	−6.84	−10.20	−10.74
	−4.27	−3.00	−5.45	−11.34	−14.70	−15.24
AbsHCla	3.26	2.08	0.43	−6.84	−10.20	−10.20
	0.83	−0.36	−1.98	−11.34	−14.70	−14.70
AddC2Cla	−2.57	−2.49	−4.15	−17.57	−16.16	−16.99
	−2.38	−2.30	−3.93	−16.07	−14.66	−15.48
AddC2Clb	−3.83	−3.63	−5.43	−18.26	−16.70	−17.60
	−3.24	−3.04	−4.82	−16.62	−15.06	−15.95
AddC3Cl	−3.89	−3.82	−5.43	−17.70	−16.89	−17.77
	−3.30	−3.23	−4.81	−15.61	−14.80	−15.69

[a]Upper value is without zero point correction, and the lower, with zero point correction.

Table 5. Relative Energies of Different Transition States (TS) and Corresponding Products, Calculated for the OH + PA Reaction[a]

	TS energies (kcal mol⁻¹)			product energies (kcal mol⁻¹)		
	MP2	QCISD	QCISD(T)	MP2	QCISD	QCISD(T)
AbsOH	9.16	4.15	2.04	−29.87	−28.57	−29.40
	7.86	2.85	0.74	−30.53	−29.22	−30.05
AddC2OHa	3.33	2.09	0.07	−36.40	−30.96	−31.66
	5.23	3.99	1.97	−31.81	−26.38	−27.08
AddC2OHb	−8.28	−2.81	−5.23	−37.90	−32.22	−33.00
	−5.77	−0.29	−2.71	−33.07	−27.39	−28.18
AddC3OH	3.64	2.50	0.04	−35.08	−30.20	−31.07
	6.05	4.91	2.45	−29.77	−24.89	−25.75

[a]Upper value is without zero point correction, and the lower, with zero point correction.
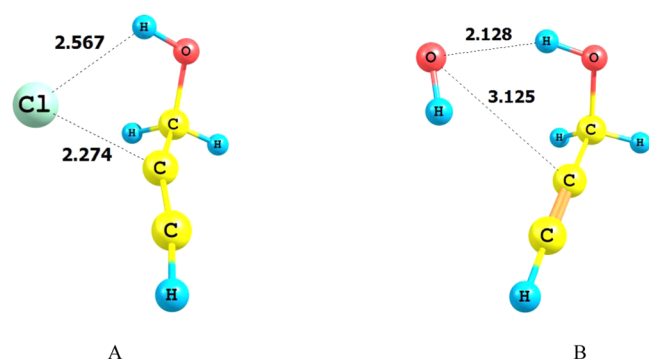
Figure 5. Optimized geometries of the probable prereactive complexes for (A) Cl reaction and (B) OH reaction.

The temperature dependence of the calculated rate coefficients, which are closest to the experimental values (at QCISD level with no correction, for Cl, and at QCISD(T) level with Wigner correction, for OH), are plotted in Figure 6. The overall rate coefficients show a decrease with increasing temperature up to about 900 K in Cl reaction and up to about 650 K in OH reaction. This probably implies the prereactive complex of Cl reaction to be more stable than that of the OH reaction. It can be seen that the ratio of abstraction to addition, which is about 1 at room temperature, changes to 2 at 1000 K for Cl reaction and from 0.2 to more than 10 in the case of the OH reaction. The significant contribution of abstraction in the Cl reaction at room temperature is similar to that of propyne, where the experimental HCl yield is reported to be about 70% at 293 K[45] and abstraction is found to be the

Table 6. Computed Rate Coefficients for Abstraction and Addition Pathways for the Reaction of Cl Atom with PA, at QCISD and QCISD(T) Levels of Calculations at 298 K[a]

TS	QCISD		QCISD(T)	
	HO	WTC	HO	WTC
AbsCl	1.57×10^{-10}	3.06×10^{-10}	9.85×10^{-9}	1.92×10^{-8}
AddC2Cla	2.31×10^{-11}	4.92×10^{-11}	3.64×10^{-10}	7.76×10^{-10}
AddC2Clb	5.05×10^{-11}	9.68×10^{-11}	1.01×10^{-9}	1.94×10^{-9}
AddC3Cl	3.02×10^{-10}	6.11×10^{-10}	4.4×10^{-9}	8.9×10^{-9}
k_{total}	6.53×10^{-10}	1.30×10^{-9}	2.48×10^{-8}	4.88×10^{-8}

[a]HO: harmonic oscillator, without any tunnelling correction. WTC: Wigner's tunneling correction. $k_{total} = k_{AddC2Clb} + k_{AddC3Cl} + 2k_{abs}$. The unit of k is cm³ molecule⁻¹ s⁻¹.

Table 7. Computed Rate Coefficients for Abstraction and Addition Pathways for the Reaction of the OH Atom (k_{OH}) with PA, at QCISD and QCISD(T) Levels of Calculations, at 298 K[a]
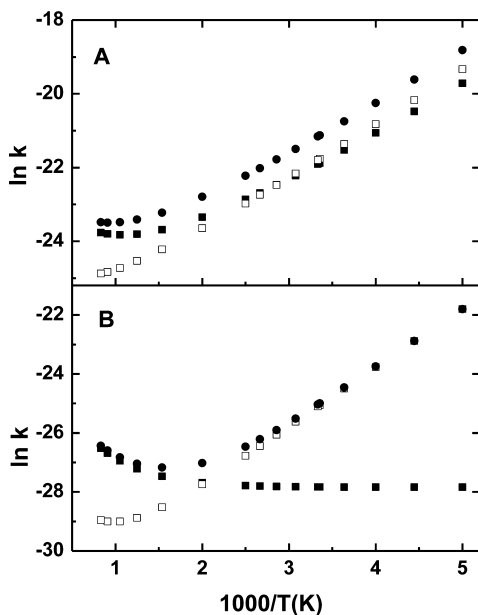
	QCISD				QCISD(T)			
TS	HO	WTC	ESTC	EUTC	HO	WTC	ESTC	EUTC
AbsOH	1.83×10^{-15}	1.16×10^{-14}	1.25×10^{-14}	1.48×10^{-13}	6.42×10^{-14}	4.08×10^{-13}	4.53×10^{-13}	2.00×10^{-12}
AddC2OHa	7.37×10^{-17}	1.01×10^{-16}	1.04×10^{-16}	1.10×10^{-16}	$2.23x\ 0^{-15}$	3.08×10^{-15}	3.16×10^{-15}	3.31×10^{-15}
AddC2OHb	3.98×10^{-14}	2.2×10^{-13}	2.54×10^{-13}	4.52×10^{-13}	2.38×10^{-12}	1.31×10^{-11}	1.91×10^{-11}	5.64×10^{-12}
AddC3	2.14×10^{-17}	3.18×10^{-17}	3.25×10^{-17}	3.62×10^{-17}	1.36×10^{-15}	2.03×10^{-15}	2.09×10^{-15}	2.29×10^{-15}
k_{total}	4.35×10^{-14}	2.43×10^{-13}	2.79×10^{-13}	7.48×10^{-13}	2.51×10^{-12}	1.39×10^{-11}	2.00×10^{-11}	9.65×10^{-12}

[a]HO: harmonic oscillator, without any tunnelling correction. WTC: Wigner's tunneling correction. ESTC: Eckart's symmetrical tunneling correction. EUTC: Eckart's unsymmetrical tunneling correction, considering the pre-reactive complex in Figure 5B. $k_{total} = k_{AddC2OHb} + 2k_{abs}$. The unit of k is cm^3 molecule^{-1} s^{-1}.

Figure 6. Variation of the computed rate coefficients with temperature for (A) Cl (computed with QCISD without any correction) and (B) OH (computed with QCISD(T) with Wigner's tunneling correction: (□) addition, (■) abstraction, and (●) total rate coefficients.

only channel at $\geq$500 K.[45,46] Thus, the abstraction reaction seems to be a dominant channel in the Cl atom reaction of triple-bonded molecules at room temperature.

The comparison of Tables 4 and 5 shows the energies of the transition states of Cl reaction to be lower than that of the OH reaction, resulting in higher rate coefficients for Cl reactions. However, the activation energy (E_a), estimated from the linear Arrhenius behavior in the temperature range 200−400 K, as seen in Figure 6, is more negative for the OH reaction (−3.7 kcal/mol) than for the Cl reaction (−2.7 kcal/mol), whereas the pre-exponential factor is an order of magnitude higher for Cl reactions. Recently, an expression for the rate coefficient of H abstraction reaction by a Cl atom at 298 K has been developed,[47] as a function of enthalpy of the reaction and Hammet parameters together, and this has been compared with that of OH.[48] In many cases, for similar experimental activation energies, the rate coefficient for OH abstraction reaction is an order of magnitude lower than that of the Cl reaction, suggested to be due to lower pre-exponential factors.[47,48] It concludes that higher reactivity of Cl atom compared to that of OH, with highly reactive substrates, results from a higher pre-exponential factor, and in less reactive substrates, the effect of activation energy dominates. The comparison of calculated rate

coefficients of reactions of OH and Cl with TAs, as discussed above, seems to support similar dominance of pre-exponential factor in the addition reaction also.

2-Propynal has been identified as one of the products of reaction of PA with Cl atom in the presence of air, identified by mass spectrometry, supporting the occurrence of the abstraction reaction. Products of addition reactions, containing the Cl atom, could not be observed consistently under our experimental conditions, even though many columns with different polarities were used. The addition of OH at the terminal carbon in the case of propyne yields formic acid, along with a radical containing carbonyl group, via a cyclic four-membered or three-membered peroxy radical.[49,50] Similar addition of Cl to PA is expected to give formyl chloride. Formic acid was observed to be one of the products, which probably is formed from formyl chloride, due to its hydrolysis by water or OH groups adhering to the surface of the vessel. The recent high level quantum chemical calculations on H abstraction reaction of Cl with ester show the rate coefficients computed by TST to be 3 orders of magnitude higher than the experimental values at low temperatures.[51] In the present case, the experimental rate coefficient at 298 K matches well with the theoretically computed overall rate coefficient. This, along with the experimental observation of abstraction products indicate the rate coefficient of H abstraction from TA, computed using conventional TST in the present study, to be not far from the actual value. However, further VTST calculations, along with quantitative analysis of products, including HCl, are desired to establish the relative significance of addition and abstraction in the Cl-initiated oxidation of these molecules. Addition is known to be the only significant channel of reaction of OH with propyne. The possibility of occurrence of H abstraction in the reaction of OH with PA, as suggested from the TST calculations applying Eckart's unsymmetrical correction, is yet to be explored experimentally.

3.3. Atmospheric Implication. The reported rate coefficient of reaction of OH with PA[17] (9.2×10^{-12} cm^3 molecule^{-1} s^{-1}) is very similar to that estimated by the AOPWIN program (10.4×10^{-12} cm^3 molecule^{-1} s^{-1}) and estimates the average tropospheric lifetime as 18 h, considering the 24 h average concentration of OH as 1×10^6 molecules cm^{-3}.[16] In the conditions of the marine boundary layer, where the Cl atom concentration can reach 1.3×10^5 molecules cm^{-3}, the tropospheric lifetime with respect to Cl atom reaction is calculated to be 6 h. Thus, even after considering the average day time concentration of OH as 2×10^6 molecules cm^{-3}, the Cl reaction is more significant than the OH reaction under the marine boundary layer conditions. Considering the fact that the rate coefficient of abstraction reaction of OH is very small, the

value of k_{OH} is expected to be similar for the other TAs, implying similar, but marginally lower, contribution of the Cl reaction in their tropospheric degradation also.

4. CONCLUSION

The present experimental determination of k_{Cl} of the triple-bonded alcohols shows their rate coefficients to be similar to that of the analogous double-bonded alcohols. This is different from the trend in k_{OH} or k_{O_3}, where the triple-bonded molecules show lower reactivity. The reactivity of PA, the simplest among TAs, with Cl and OH is examined theoretically at the same level of calculation, using the same basis set, and compared. Exothermicity of the reaction does not play much of a role in deciding the rate coefficients. The TS energy for abstraction of an H atom, α to the alcoholic group, is found to be lower for the Cl reaction than for the OH reaction. The addition reactions at both terminal and middle carbon atoms have submerged TS in the case of Cl, with the terminal one being more negative, whereas only the addition at the middle carbon has submerged TS in the case of the OH reaction. Thus, the dominant site of addition of OH is the middle carbon, whereas that of Cl is the terminal carbon. There is significant contribution of abstraction in the Cl reaction at room temperature, but not in the OH reaction. The logarithmic plot of the theoretically calculated rate coefficients shows a linear variation with temperature, with inverse Arrhenius behavior in the 200−400 K range. The slopes of the addition rate coefficients correspond to negative activation energies of 2.7 and 3.6 kcal/mol in reactions of Cl and OH, respectively. The pre-exponential factor for Cl is found to be about an order of magnitude higher than that of OH, for both abstraction and addition channels. This is very similar to the observation in saturated molecules, where the major factor responsible for the higher rate coefficient of the Cl reaction than for the OH reaction is concluded to be the pre-exponential factor, not the activation energy.

■ ASSOCIATED CONTENT

Ⓢ Supporting Information

Structural parameters in the form of Cartesian coordinates and vibrational frequencies of all the optimized geometries are given. This material is available free of charge via the Internet at http://pubs.acs.org.

■ AUTHOR INFORMATION

Corresponding Author
*S. Dhanya. E-mail: sdhanya@barc.gov.in. Tel: 0091-22-25593760. Fax: 91-22-25505151.

Notes
The authors declare no competing financial interest.

■ ACKNOWLEDGMENTS

■ REFERENCES

(1) Atkinson, R. Kinetics and mechanisms of the gas-phase reactions of the hydroxyl radical with organic compounds under atmospheric conditions. *Chem. Rev.* **1986**, *86*, 69−201.

(2) Kwok, E. S. C.; Atkinson, R. Estimation of hydroxyl radical reaction rate Constants for gas-phase organic compounds using a structure-reactivity relationship: An update. *Atmos. Environ.* **1995**, *29*, 1685−1695.

(3) King, M. D.; Canosa-Mas, C. E.; Wayne, R. P. A structure−activity relationship (SAR) for predicting rate constants for the reaction of NO_3, OH and O_3 with monoalkenes and conjugated dienes. *Phys. Chem. Chem. Phys.* **1999**, *1*, 2239−2246.

(4) Pfrang, C.; King, M. D.; Braeckevelt, M.; Canosa-Mas, C. E.; Wayne, R. P. A structure-activity relationship (SAR) for predicting rate constants for the reaction of OH, NO_3, and O_3 with monoalkenes and conjugated dienes. *Atmos. Environ.* **2008**, *42*, 3018−3034.

(5) Spicer, C. W.; Chapman, E. G.; Finlayson-Pitts, B. J.; Plastridge, R. A.; Hubbe, J. M.; Fast, J. D.; Berkowitz, C. M. Unexpectedly high concentrations of molecular chlorine in coastal air. *Nature* **1998**, *394*, 353−356.

(6) Thornton, J. A.; Kercher, J. P.; Riedel, T. P.; Wagner, N. L.; Cozic, J.; Holloway, J. S.; Dube, W. P.; Wolfe, G. M.; Quinn, P. K.; Middlebrook, A. M.; et al. A large atomic chlorine source inferred from mid-continental reactive nitrogen chemistry. *Nature* **2010**, *464*, 271−274.

(7) Sharma, A.; Pushpa, K. K.; Dhanya, S.; Naik, P. D.; Bajaj, P. N. Rate coefficients and products of gas-phase reactions of chlorine atoms with cyclic unsaturated hydrocarbons at 298 K. *Int. J. Chem. Kinet.* **2010**, *42*, 98−105.

(8) Sharma, A.; Pushpa, K. K.; Dhanya, S.; Naik, P. D.; Bajaj, P. N. Rate constants for the gas-phase reactions of chlorine atoms with 1,4-cyclohexadiene and 1,5-cyclooctadiene at 298 K. *Int. J. Chem. Kinet.* **2011**, *43*, 431−440.

(9) Walavalkar, M. P.; Sharma, A.; Alwe, H. D.; Pushpa, K. K.; Dhanya, S.; Naik, P. D.; Bajaj, P. N. Cl atom initiated oxidation of 1-alkenes under atmospheric conditions. *Atmos. Environ.* **2013**, *67*, 93−100.

(10) Alwe, H. D.; Walavalkar, M. P.; Sharma, A.; Pushpa, K. K.; Dhanya, S.; Naik, P. D. Rate coefficients for the gas-phase reactions of chlorine atoms with cyclic ethers at 298 K. *Int. J. Chem. Kinet.* **2013**, *45*, 295−305.

(11) Alwe, H. D.; Walavalkar, M. P.; Sharma, A.; Dhanya, S.; Naik, P. D. Tropospheric oxidation of cyclic unsaturated ethers in the day-time: comparison of the reactions with Cl, OH and O_3 based on the determination of their rate coefficients at 298 K. *Atmos. Environ.* **2014**, *82*, 113−120.

(12) Carey, F. A.; Sundberg, R. J. *Advanced organic chemistry*, 5th ed.; Springer: New York, 2007.

(13) Atkinson, R.; Aschmaan, S. M. Rate constants for the reactions of O_3 and OH radicals with a series of alkynes. *Int. J. Chem. Kinet.* **1984**, *16*, 259−268.

(14) Holme, A.; Sæthre, L. J.; Børve, K. J.; Thomas, T. D. Chemical reactivity of alkenes and alkynes as seen from activation energies, enthalpies of protonation, and carbon 1s ionization energies. *J. Org. Chem.* **2012**, *77*, 10105−10117.

(15) Atkinson, R.; Baulch, D. L.; Cox, R. A.; Crowley, J. N.; Hampson, R. F.; Hynes, R. G.; Jenkin, M. E.; Rossi, M. J.; Troe, J. *Atmos. Chem. Phys.* **2004**, *4*, 1461−1738. IUPAC subcommittee for gas kinetic data evaluation, http://iupac.pole-ether.fr. vol. *2* IUPAC (accessed 10-07-2014).

(16) U.S. EPA HPV Challenge Program Revised Submission on propargyl alcohol, dated July 30, 2003; Publication 201-14641A, http://www.epa.gov/hpv/pubs/summaries/propargy/c14222rs.pdf.

(17) Upadhyaya, H. P.; Kumar, A.; Naik, P. D.; Sapre, A. V.; Mittal, J. P. Kinetics of OH radical reaction with allyl alcohol ($H_2C=CHCH_2OH$) and propargyl alcohol ($HC\equiv CCH_2OH$) studied by LIF. *Chem. Phys. Lett.* **2001**, *349*, 279−285.

(18) Thiebaud, J.; Aluculesei, A.; Fittschen, C. Formation of HO_2 radicals from the photodissociation of H_2O_2 at 248 nm. *J. Chem. Phys.* **2007**, *126*, 186101−2.

(19) Manion, J. A.; Huie, R. E.; Levin, R. D.; Burgess Jr., D. R.; Orkin, V. L.; Tsang, W.; McGivern, W. S.; Hudgens, J. W.; Knyazev, V. D.; Atkinson, D. B.; et al. NIST Chemical Kinetics Database, NIST

Standard Reference Database 17, Version 7.0 (Web Version), Release 1.4.3, Data version 2008.12; National Institute of Standards and Technology: Gaithersburg, MD 20899-8320. Web address: http://kinetics.nist.gov/.

(20) Finlayson-Pitts, B. J.; Keoshian, C. J.; Buehler, B.; Ezell, A. A. Kinetics of reactions of chlorine atom with some biogenic organics. *Int. J. Chem. Kinet.* **1999**, *31*, 491−499.

(21) Oyeyemi, V. B.; Keith, J. A.; Pavone, M.; Carter, E. A. Insufficient Hartree−Fock exchange in hybrid DFT functionals produces bent alkynyl radical structures. *J. Phys. Chem. Lett.* **2012**, *3*, 289−293.

(22) Bode, B. M.; Gordon, M. S. Macmolplt: a graphical user interface for GAMESS. *J. Mol. Graphics Modell.* **1998**, *16*, 133−138.

(23) Rodríguez, A.; Rodríguez, D.; Garzón, A.; Soto, A.; Aranda, A.; Notario, A. Kinetics and mechanism of the atmospheric reactions of atomic chlorine with 1-penten-3-ol and (Z)-2-penten-1-ol: an experimental and theoretical study. *Phys. Chem. Chem. Phys.* **2010**, *12*, 12245−12258.

(24) Rodríguez, D.; Rodríguez, A.; Garzón, A.; Roldán, José M. G.; Soto, A.; Aranda, A.; Notario, A. Kinetic and mechanistic study of the atmospheric reaction of MBO331 with Cl atoms. *Mol. Phys.* **2012**, *110*, 2941−2950.

(25) Schmidt, M. W.; Baldridge, K. K.; Boatz, J. A.; Elbert, S. T.; Gordon, M. S.; Jensen, J. J.; Koseki, S.; Matsunaga, N.; Nguyen, K. A.; Su, S.; et al. General atomic and molecular electronic structure system. *J. Comput. Chem.* **1993**, *14*, 1347−1363.

(26) Frisch, M. J.; Trucks, G. W.; Schlegel, H. B.; Scuseria, G. E.; Robb, M. A.; Cheeseman, J. R.; Zakrzewski, V. G.; Montgomery Jr., J. A.; Stratmann, R. E.; Burant, J. C.; et al. *Gaussian*; Gaussian, Inc.: Pittsburgh, PA, 2001.

(27) O'Boyle, N. M.; Banck, M.; James, C. A.; Morley, C.; Vandermeersch, T.; Hutchison, G. R. Open Babel: An open chemical toolbox. *J. Chem. Inf.* **2011**, 3−33.

(28) Laidler, K. J. *Chemical kinetics*, 3rd ed.; Pearson Education: Delhi, 2004.

(29) Wigner, E. P. Über das überschreiten von potentialschwellen bei chemischen reaktionen. *Z. Phys. Chem. B* **1932**, *19*, 203.

(30) Eckart, C. The penetration of a potential barrier by electrons. *Phys. Rev.* **1930**, *35*, 1303−1309.

(31) Johnston, H. S.; Heicklen, J. Tunnelling corrections for unsymmetrical Eckart potential energy barriers. *J. Phys. Chem.* **1962**, *66*, 532−533.

(32) Ogura, T.; Miyoshi, A.; Koshi, M. Rate coefficients of H-atom abstraction from ethers and isomerization of alkoxyalkylperoxy radicals. *Phys. Chem. Chem. Phys.* **2007**, *9*, 5133−5142.

(33) Chase Jr, M. W.; Davies, C. A.; Downey, J. R., Jr.; Frurip, D. J.; McDonald, R. A.; Syverud, A. N. JANAF Thermochemical Tables, 3rd ed. *J. Phys. Chem. Ref. Data 14*, **1985**, Suppl. 1.

(34) Lee, J. H.; Hwang, H.; Kwon, C. H.; Kim, H. L. Photodissociation dynamics of 2-propyn-1-ol at 212 nm: the OH production channel. *J. Phys. Chem. A* **2010**, *114*, 2053−2058.

(35) Orlando, J. J.; Tyndall, G. S.; Apel, E. C.; Riemer, D. D.; Paulson, S. E. Rate coefficients and mechanisms of the reaction of Cl-atoms with a series of unsaturated hydrocarbons under atmospheric conditions. *Int. J. Chem. Kinet.* **2003**, *35*, 334−353.

(36) Takahashi, K.; Xing, J. H.; Hurley, M. D.; Wallington, T. J. Kinetics and mechanism of chlorine-atom-initiated oxidation of allyl alcohol, 3-buten-2-ol, and 2-methyl-3-buten-2-ol. *J. Phys. Chem. A* **2010**, *114*, 4224−4231.

(37) Liang, P.; Mu, Y. J.; Daele, V.; Mellouki, A. Kinetic studies of Cl reactions with 3-buten-1-ol and 2-buten-1-ol over the temperature range 298−363 K. *Chem. Phys. Lett.* **2011**, *502*, 154−158.

(38) Gai, Y.; Ge, M.; Wang, W. Kinetics of the gas-phase reactions of some unsaturated alcohols with Cl atoms and O_3. *Atmos. Environ.* **2011**, *45*, 53−59.

(39) Papagni, C.; Arey, J.; Atkinson, R. Rate constants for the gas-phase reactions of OH radicals with a series of unsaturated alcohols. *Int. J. Chem. Kinet.* **2001**, *33*, 142−147.

(40) Rodríguez, A.; Rodríguez, D.; Soto, A.; Notario, A.; Aranda, A.; Díaz-de-Mera, Y.; Bravo, I. Relative rate measurements of reactions of unsaturated alcohols with atomic chlorine as a function of temperature. *Atmos. Environ.* **2007**, *41*, 4693−4702.

(41) Pearson, J. C.; Drouin, B. J. The ground state torsion−rotation spectrum of propargyl alcohol ($HCCCH_2OH$). *J. Mol. Spectrosc.* **2005**, *234*, 149−156.

(42) Stewart, E. L.; Mazurek, U.; Phillip, J. Ab initio and molecular mechanics (MM3) calculations on property alcohol and derivatives. *J. Phys. Org. Chem.* **1996**, *9*, 66−78.

(43) Mani, D.; Arunan, E. Microwave spectroscopic and atoms in molecules theoretical investigations on the Ar···Propargyl alcohol complex: Ar···H-O, Ar···π, and Ar···C interactions. *Chem. Phys. Chem.* **2013**, *14*, 754−763.

(44) Zhang, Y.; Chao, K.; Sun, J.; Su, Z.; Pan, X.; Zhang, J.; Wang, R. Theoretical study on the gas phase reaction of allyl alcohol with hydroxyl radical. *J. Phys. Chem. A* **2013**, *117*, 6629−6640.

(45) Farrell, J. T.; Taatjes, C. A. Infrared frequency-modulation probing of Cl + C_3H_4 (allene, propyne) reactions: kinetics of HCl production from 292 to 850 K. *J. Phys. Chem. A* **1998**, *102*, 4846−4856.

(46) Shafir, E. V.; Slagle, I. R.; Knyazev, V. D. Kinetics and products of the self-reaction of propargyl radicals. *J. Phys. Chem. A* **2003**, *107*, 8893−8903.

(47) Poutsma, M. L. Evolution of structure−reactivity correlations for the hydrogen abstraction reaction by hydroxyl radical and comparison with that by chlorine atom. *J. Phys. Chem. A* **2013**, *117*, 6433−6449.

(48) Poutsma, M. L. Evolution of structure−reactivity correlations for the hydrogen abstraction reaction by chlorine atom. *J. Phys. Chem. A* **2013**, *117*, 687−703.

(49) Boodaghians, R. B.; Hall, I. W.; Toby, F. S.; Wayne, R. P. Absolute determinations of the kinetics and temperature dependences of the reactions of OH with a series of alkynes. *J. Chem. Soc., Faraday. Trans.* **1987**, *83*, 2073−2080.

(50) Yeung, L. Y.; Pennino, M. J.; Miller, A. M.; Elrod, M. J. Kinetics and mechanistic studies of the atmospheric oxidation of alkynes. *J. Phys. Chem. A* **2005**, *109*, 1879−1889.

(51) Chow, R.; Ng, M.; Mok, D. K. W.; Lee, E. P. F.; Dyke, J. M. Rate coefficients of the Cl + $CH_3C(O)OCH_3$ → HCl + $CH_3C(O)$-OCH_2 reaction at different temperatures calculated by transition-state theory with ab initio and density functional theory reaction paths. *J. Phys. Chem. A* **2014**, *118*, 2040−2055.